Carbon 111 (2017) 807–812

Contents lists available at ScienceDirect

Carbon

journal homepage: www.elsevier.com/locate/carbon

Super-tough artificial nacre based on graphene oxide via synergistic interface interactions of π-π stacking and hydrogen bonding

Pingan Song [a, b, c, *, 1], Zhiguang Xu [b, 1], Yuanpeng Wu [d], Qunfeng Cheng [e, **], Qipeng Guo [b, ***], Hao Wang [c]

[a] Department of Materials, College of Engineering, Zhejiang A & F University, Hangzhou, Zhejiang, 311300, China
[b] Polymers Research Group, Institute for Frontier Materials, Deakin University, Locked Bag 20000, Geelong, Victoria, 3220, Australia
[c] Centre for Future Materials, University of Southern Queensland, Toowoomba, Queensland, 4350, Australia
[d] School of Materials Science and Engineering, Southwest Petroleum University, Chengdu, Sichuan, 610500, China
[e] Key Laboratory of Bio-inspired Smart Interfacial Science and Technology of Ministry of Education, School of Chemistry Environment, Beihang University, Beijing, 100191, China

ARTICLE INFO

Article history:
Received 26 August 2016
Received in revised form
19 October 2016
Accepted 25 October 2016
Available online 26 October 2016

ABSTRACT

Inspired by interfacial interactions of protein matrix and the crystal platelets in nacre, herein, a super-tough artificial nacre was produced through constructing the synergistic interface interactions of π-π interaction and hydrogen bonding between graphene oxide (GO) nanosheets and sulfonated styrene-ethylene/butylene-styrene copolymer synthesized with multifunctional benzene. The resultant GO-based artificial nacre showed super-high toughness of 15.3 ± 2.5 MJ/m^3, superior to natural nacre and other GO-based nanocomposites. The ultra-tough property of the novel nacre was attributed to synergistic effect of π-π stacking interactions and hydrogen bonding. This bioinspired synergistic toughening strategy opens a new avenue for constructing high performance GO-based nanocomposites in the near future.

© 2016 Elsevier Ltd. All rights reserved.

1. Introduction

Natural nacre demonstrates extraordinary fracture toughness ranging to 3000 times higher than the intrinsic toughness of its constituent of $CaCO_3$ platelets. This level of toughness is attributed to the interfacial interactions between organic protein matrix and $CaCO_3$ platelets [1–3]. Inspired by this relationship of extraordinary toughness and abundant interface interactions, a range of bio-inspired nanocomposites based on different inorganic platelets have been demonstrated, including flattened double-walled carbon nanotubes [4], man-made $CaCO_3$ [5,6], nanoclay [7,8], Al_2O_3 flakes [9,10], and layered double hydroxides [11]. Graphene oxide (GO) nanosheets with numerous oxygen-containing groups are an ideal candidate for achieving the artificial nacre construction through the design of different interface interactions, including hydrogen bonding, ionic bonding, π-π interaction, and covalent bonding. Many GO-based artificial nacre with excellent mechanical properties have been produced by constructing different interface interactions [12–18], for example, the GO-Borate, *r*GO-PCDO, PGO-PDA, *r*GO-SL, and *r*GO-PAPB. In our previous report [16,17], we demonstrated ultra-tough GO-based artificial nacre with long linear molecules of PCDO, which absorbs much energy when the coiled structure is stretched under loading. However, constructing much tougher GO-based artificial nacre remains a great challenge.

Recently, our group has developed a new route to toughen brittle epoxy thermosets with the block ionomer, sulfonated polystyrene-*block*-poly (ethylene-*co*-butylene)-*block*-polystyrene (SSEBS) via sulfonating polystyrene-*block*-poly (ethylene-*co*-butylene)-*block*-polystyrene (SEBS) with 67 wt% of polystyrene (PS) [19,20]. Moreover, styrene segments in SEBS can form strong π-π stacking [21] whereas sulfoacid groups can form hydrogen bonds with oxygen-containing groups on the GO surface, which can guarantee strong interfaces between GO and SSEBS and thus facilitate the stress transfer and energy dissipation upon external load.

* Corresponding author. Department of Materials, College of Engineering, Zhejiang A & F University, Hangzhou, Zhejiang, 311300, China.
** Corresponding author.
*** Corresponding author.
E-mail addresses: pingansong@gmail.com (P. Song), cheng@buaa.edu.cn (Q. Cheng), qguo@deakin.edu.au (Q. Guo).
[1] P. Song and Z. Xu contributed equally to the work.

http://dx.doi.org/10.1016/j.carbon.2016.10.067
0008-6223/© 2016 Elsevier Ltd. All rights reserved.

Table 1
Loading level of polymers and *d*-spacing for as-prepared artificial nacre.

Run	Loading level of polymer (wt%)		*d*-spacing (Å) by XRD
	Input	by TGA	
GO	–	–	7.21
GO-S-2	2.0	1.90	7.34
GO-S-5	5.0	4.90	7.72
GO-S-10	10	9.90	8.85
GO-S-15	15	14.8	9.01
GO-S-20	20	19.7	9.27

In this work, we have demonstrated super-tough GO-based artificial nacre through synergistic toughening of π-π interaction and hydrogen bonding. A new water-soluble long chain molecule, sulfonated styrene-ethylene/butylene-styrene (SSEBS), with many benzene groups was synthesized through sulfonating SEBS triblock copolymers. Then the SSEBS and GO nanosheets were assembled into artificial nacre via vacuum assisted-filtration. The strong π-π interaction is formed between the benzene groups with GO nanosheets, and hydrogen bonding network is formed between hydroxyl groups, carboxyl groups of GO nanosheets, and sulfonic groups of SSEBS [19–21] as well. The resultant synergistic effect of π-π interactions and hydrogen bonding improves the efficiency of stress transfer, and long soft SSEBS segments easily deform and extend under loading, dissipating much more fracture energy. The toughness of GO-SSEBS reaches as high as 15.3 MJ/m^3, which is eight times higher than that of natural nacre [22], and superior to other GO-based artificial nacre. This bioinspired synergistic toughening of π-π interactions and hydrogen bonding strategy opens a new avenue for constructing high performance GO-based nanocomposites in the near future.

2. Experimental section

2.1. Materials

Graphene oxide (GO) was prepared according to our previous work [23]. Detailed preparation process of sulfonated styrene-ethylene/butylene-styrene (SSEBS) is provided in Supporting Information.

2.2. Fabrication of SSEBS-toughened GO-based artificial nacre

Firstly, 1.5 g of each polymer (GO, SSEBS) was dispersed in 1000 ml deionized water with the aid of sonication for 30 min, and then stirring for 3 h and to prepare 1.5 mg/ml aqueous solutions of GO, and SSEBS, respectively. Then, a certain amount of SSEBS solution was added into the GO solution according to desired mass ratios. The mixtures were then stirred for 12 h to form a homogeneous solution. Finally, the SSEBS-intercalated GO-based artificial nacre was obtained with vacuum-assisted filtration self-assembly process. Additionally, the GO-PVA film was prepared using the same preparation protocol to GO-SSEBS but according to the ratio, 50 wt% PVA, in previous reports as a comparison to evaluate the advantage of SSEBS over PVA as the intercalating agent. Detailed formulations and sample designation are shown in Table 1.

2.3. Characterization

Typical tapping-mode atomic force microscopy (AFM) measurements were performed on a Bruker Multi Mode 8 SPM instrument (USA). Scanning electron microscopy (SEM) images were obtained using a field-emission scanning electron microscope (FEI-SEM S4800) at an acceleration voltage of 5 kV. The accelerating voltage was increased up to 15 kV for energy dispersive X-ray spectroscopy (EDX) measurements. XPS measurements were performed using ESCAlab 250XI electron spectrometer. X-ray diffraction (XRD) tests were carried out using a Rigaku X-ray generator (Cu K_α radiation). Infrared (IR) spectra of all films were recorded on a Bruker Vetex-70 IR spectrometer (Germany) using an attenuated total reflectance (ATR) mode. Raman spectra were obtained with an ALMEGA-Dispersive Raman (Thermo Nicolet) with 514.5 nm excitation. Thermogravimetric analysis (TGA) was conducted on a TA Q50 thermal analyzer (TGA, USA) in a temperature range of 50–750° C in nitrogen with a heating rate of 5 °C/min. Mechanical properties were measured using an Instron 30 kN tensile tester at 23 ± 2 °C at a loading rate of 1 mm/min with a gauge length of

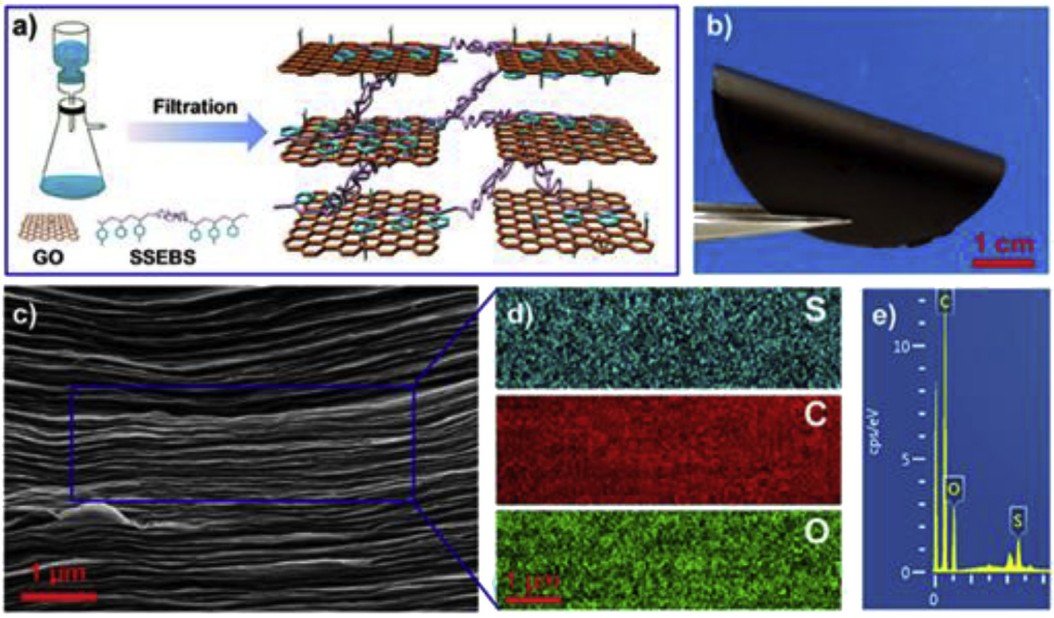

Fig. 1. (a) Schematic representation of the fabrication process of GO-S-n artificial nacre via vacuum-assisted filtration. (b) Digital photograph and (c) Cross-section morphology of GO-S-10. (d) Elemental maps and (e) Elemental composition of GO-S-10. (A colour version of this figure can be viewed online.)

10 mm. All of the samples were cut into strips with a length of 40 mm and a width of 2 mm width before measurement. The results for each sample ware based on the average value of at least 5 specimens.

3. Results and discussion

The size of GO nanosheets is in the range of 1.0–5.0 μm with a thickness of ~1 nm (Figure S1), and the water-soluble SSEBS was synthesized via sulfonating SEBS (Scheme S1). After sulfonation, four new absorption peaks appear in the infrared spectrum (IR), respectively locating at 3397 cm^{-1} (the stretching vibration of O–H in $-SO_3H$), 1126 cm^{-1}, 1032 cm^{-1} and 1003 cm^{-1} (stretching vibration of S–O) [24,25] (Figure S2A). Elemental analysis results show that SSEBS contains 5.14 wt% S element, and the aqueous solution of 5.0 wt% SSEBS looks brown and transparent (Figure S2B), revealing the water-solubility of SSEBS. The GO-SSEBS artificial nacre is assembled via vacuum-assisted filtration, as shown in Fig. 1a. 1.0 wt% GO suspension was prepared by dispersing the GO nanosheets into deionized water with the aid of sonication and stirring, and then the 1.0 wt% aqueous solution of SSEBS was added. The mixture was further stirred for 12 h, and filtrated with vacuum-assistance. Different SSEBS content of resultant artificial nacre were fabricated for comparison, and the resultant artificial nacre were designated as GO-S-n, in which n represents the SSEBS content. In this study, five kinds of artificial nacre are fabricated, listed as: GO-S-2, GO-S-5, GO-S-10, GO-S-15, and GO-S-20. The real content of SSEBS is further confirmed, as shown in Fig. S5 and listed in Table S1. The digital photograph of flexible GO-S-10 is shown in Fig. 1b. Cross-section morphology of GO-S-10 indicates clearly well orderly nacre-mimetic structure, as shown in Fig. 1c. The elemental map reveals uniform dispersion of presence of C, O and S (2.38 wt%) elements, as shown in Fig. 1d–e.

To further verify the presence of SSEBS in the gallery of adjacent GO nanosheets, X-ray photoelectron spectroscopy (XPS) tests were conducted. Besides typical binding energy peaks for pure GO (Fig. S3), a new peak at 286.9 eV belonging to the binding energy of C–S bonds appears in the C1s spectrum of GO-S-10, as shown in Fig. 2a, and the content of S element was determined to be 2.42 wt% (Fig. S4). Raman spectra demonstrate that the I_D/I_G ratio value

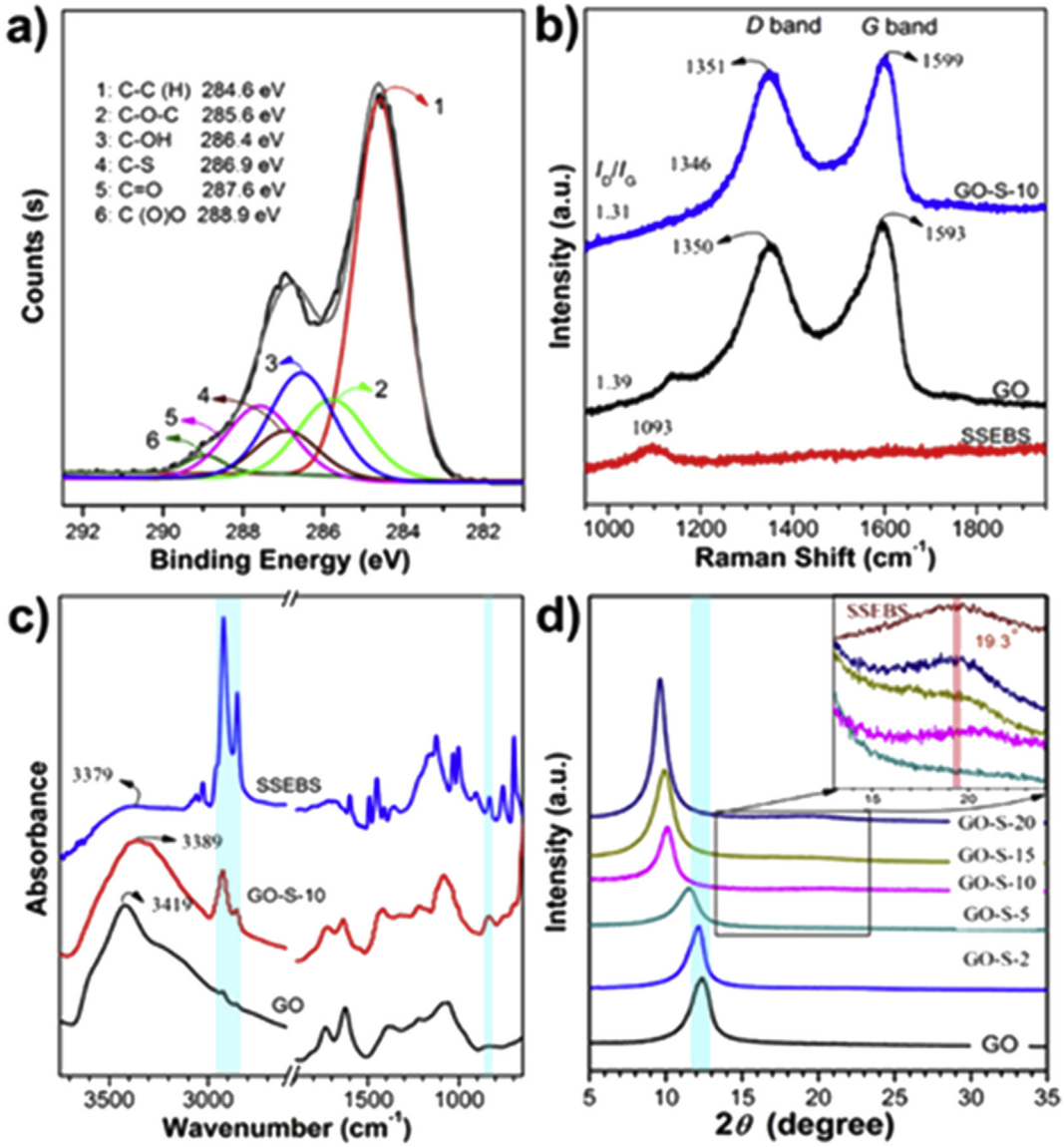

Fig. 2. (a) C1s spectrum of GO-S-10, (b) Raman spectra of SSEBS, pure GO, GO-S-10, and GO-S-50. Appearance of binding energy peaks at 232.7eV (S2s) and 168.9 eV (S2p) together with the peak belonging to C–S (286.8 eV) suggests SSEBS was successfully introduced into GO galleries. (c) FTIR spectra of pure GO, GO-S-10 and SSEBS. (d) XRD spectra of pure GO, GO-S-2, GO-S-5, GO-S-10, GO-S-15, and GO-S-20, respectively. (A colour version of this figure can be viewed online.)

decreases from 1.39 for pure GO to 1.31 for GO-S-10, as shown in Fig. 2b. Moreover, though pristine SSEBS only exhibits a band at 1093 cm^{-1}, adding SSEBS makes *G* band (1593 cm^{-1}) for pure GO shift to higher wave-numbers (~1599 cm^{-1}), mainly because of the strong π-π interactions between GO nanosheets and SSEBS [21]. In comparison, introducing PVA causes *G* and *D* bands to shift to lower wave-numbers (1588 and 1346 cm^{-1}). In addition, two new absorption peaks at 2930 and 2856 cm^{-1} (stretching vibrations of CH_2 in SSEBS chains) appear in the IR spectrum of GO-S-10, further indicating the presence of SSEBS in the gallery of adjacent GO nanosheets (Fig. 2c).

X-ray diffraction (XRD) measurements were carried out to determine the interlayer distance (*d*-spacing) of the resultant the interlayer distance artificial nacres. As shown in Fig. 2d and Table S1, pure GO film displays a small *d*-spacing of 7.21 Å. After introducing SSEBS, the *d*-spacing value of artificial nacre steadily increases with increasing polymer loading level, for instance, a *d*-spacing of 7.34 Å for GO-S-2, 7.72 Å for GO-S-5, 8.85 Å for GO-S-10, 9.01 Å for GO-S-15, and 9.27 Å for GO-S-20. The gradually increasing *d*-spacing strongly further indicates the successful intercalating of SSEBS into gallery of the adjacent GO nanosheets. Moreover, upon the input SSEBS content above 10 wt%, the diffraction peak at about 19.3° corresponding to characteristic peak of SSEBS appears.

Typical stress-strain curves of GO-S-n artificial nacre are shown in Fig. 3a. The presence of small amount of SSEBS causes GO nanosheets to exhibit remarkably enhanced tensile strength and extensibility due to strong interfacial interactions between GO nanosheets and SSEBS as well as high deformation capabilities of SSEBS. As shown in curve 1 of Fig. 3a, the pure GO film displays a tensile strength of about 90 MPa and toughness of 1.53 MJ/m^3, consistent with previous reports [16–18]. The pure SSEBS film exhibits a much lower tensile strength of about 14 MPa, but a much higher strain of 100% (Table S1).

The tensile strength and toughness of GO-S-n artificial nacre, steadily increase with increasing SSEBS content, and reach the maximum values when the SSEBS content is about 10 wt% (GO-S-10). The tensile strength and toughness of GO-S-10 reach up to 158 ± 6.0 MPa and 15.3 ± 1.5 MJ/m^3, corresponding to 76% and 900% improvement compared to that of pure GO film, respectively.

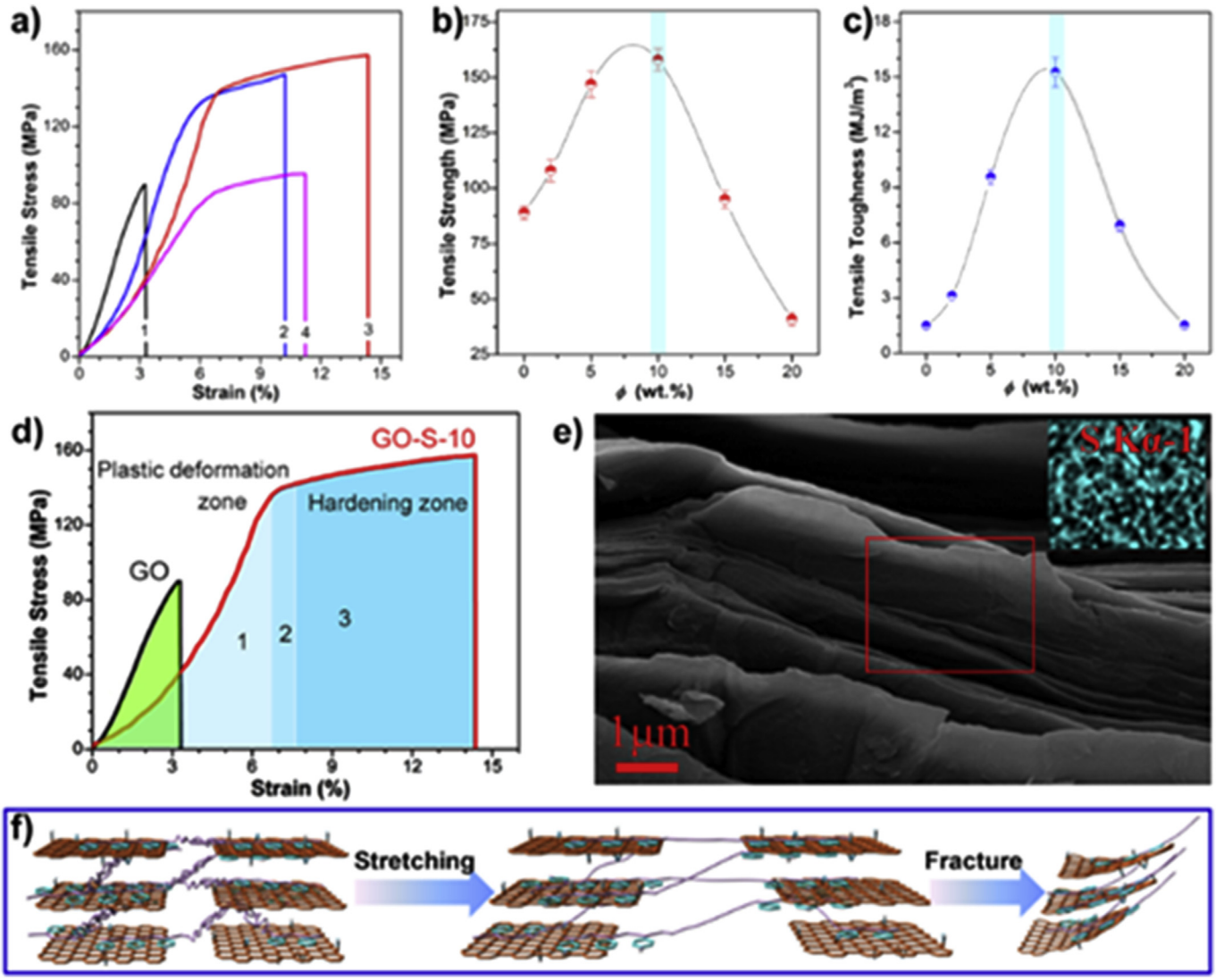

Fig. 3. (a) Typical stress-strain curves of pure GO film (curve 1), GO-S-5 (curve 2), GO-S-10 (curve 3), and GO-S-15 (curve 4). (b) Tensile strength and (c) toughness of GO and GO-S-n artificial nacre with different SSEBS content, indicating that both tensile strength and toughness reach the maximum value at a SSEBS content of about 10 wt%. (d) Typical stress-strain curve of the pure SSEBS film and GO-S-10 artificial. (e) Fracture morphology of GO-S-10 artificial nacre after tensile testing. (f) Proposed fracture mechanism of GO-S-10 artificial nacre. (A colour version of this figure can be viewed online.)

However, when the SSEBS content further increases, the tensile strength and toughness dramatically decreases, as shown in Fig. 3b–c. When the SSEBS content is lower than 10 wt%, the presence of SSEBS cannot provide enough space for the mutual slippage of GO nanosheets, which limits the dissipation of energy in process of fracturing of π-π interactions, deforming and extending of SSEBS under loading. However, when the SSEBS content is higher than 10 wt%, the excess SSEBS probably only acts as the intercalating impurity to increase both the interlayer spacing and the area of cross-section of GO-S-n artificial nacre. Meanwhile, the excess SSEBS may also hinder the stress transfer between adjacent GO nanosheets, which is also observed by previous report [18]. Detailed mechanical properties of other GO-S-n artificial nacre are listed in Table S1.

Compared to the pure GO film, the artificial nacre of GO-S-10 exhibits a typical stress-strain curve with two failure stages, including the elastic deformation, and hardening stage, as shown in Fig. 3d. This is because that there are numerous interface interactions between GO nanosheets and SSEBS. For example, π-π interactions are formed between GO nanosheets and long polystyrene (PS) segments in SSEBS, and the hydrogen bonding are formed between sulfonic acid groups on PS segments with abundant hydroxyl, carboxyl groups on the surface of GO nanosheets. The proposed fracture process is illustrated as show in Fig. 3f. Taking the artificial nacre of GO-S-10 as an example, the corresponding stress-strain curve is shown in Fig. 3d. When the loading starts, the GO-S-10 artificial nacre first show the plastic deformation, designated as stage I, the soft long aliphatic chains of EB segments in SSEBS start to deform and extend from the randomly coiled conformation between adjacent GO nanosheets, resulting in large strain. This form of plasticization facilitates the mutual slippage of GO nanosheets upon loading, which also results in high dissipation of energy. When continuously stretching, EB chains further extend along the direction of stretching. Then, the stage II of the hardening stage starts, and the EB chains are stretched to uncoil until fracture. In this process, firstly, the hydrogen bonds fracture, and then the π-π stacking interactions begin to rupture with increasing loading. Finally, a fraction of GO nanosheets are pulled out, as shown in Fig. 3e. The S element is detected on the pulled out GO nanosheets, indicating that SSEBS is also pulled out with GO nanosheet in the facture process, mainly because of the strong π-π stacking interactions between SSEBS and GO nanosheets.

This form of artificial nacre shows super high toughness compared to natural nacre and other GO-based nanocomposites, and the comparison of stress strain curves is shown in Fig. 4, with detailed mechanical properties listed in Table S2. The artificial nacre of GO-S-10 exhibits toughness of 15.3 MJ/m^3, which is almost about 8.5 times of that of natural nacre with 1.8 MJ/m^3, and other GO-based nanocomposites with different cross-linking strategies. For example, Tian et al. [26] applied polyetherimide (PEI) cross-link GO nanosheets and achieved strong GO-based nanocomposites (GO-PEI) with tensile strength of ~209.9 MPa, but low toughness of 0.23 MJ/m^3, and the corresponding stress-strain curve is shown in curve 10 of Fig. 4. This behavior is because of the strong covalent bonding, which limits the mutual slippage of adjacent GO nanosheets resulting in high strength but low toughness. The other GO-based nanocomposites with covalent bonding, such as GO-PAA, GO-GA, GO-PDA, GO-Borate, and GO-PCDO, also demonstrate the high tensile strength but low toughness. For GO-based nanocomposites with ionic bonding, such as GO-Mg^{2+} and GO-Ca^{2+}, the enhancements in toughness and strength are also difficult. On the other hand, although the tensile strength of polymer reinforced GO nanosheets nanocomposites show high strength, they exhibit low toughness because of weak interactions, such as GO-PMMA, GO-PVA, GO-MoS_2-TPU, and GO-Al_2O_3-PVA. Recently, the high toughness graphene-based nanocomposites are achieved through chemically reducing the GO-based nanocomposites, for example, GO-CS, GO-CNC, and GO-HPG. In this study, we focused primarily on the GO-based nanocomposites.

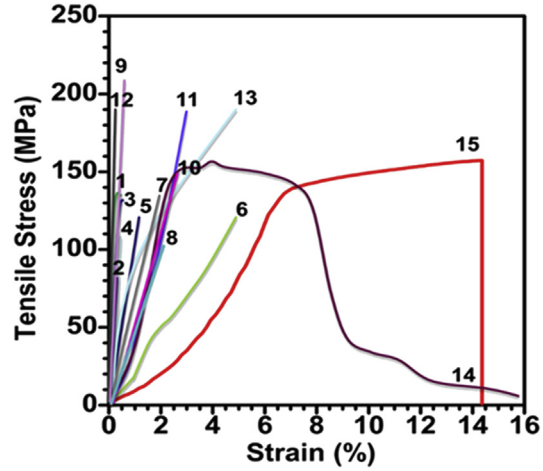

Fig. 4. Comparison of stress-strain curves with GO-S-10 artificial nacre (Curve 15) with other GO-based nanocomposites, such as GO-Mg^{2+} (Curve 2) [27], GO-Ca^{2+} (Curve 3) [27], GO-PAA (Curve 4) [28], GO-PVA (Curve 5) [29], GO-PCDO (Curve 6) [16], GO-SF (Curve 7) [30], GO-GA (Curve 8) [31], GO-PEI (Curve 9) [26], GO-PMMA (Curve 10) [32], GO-PDA (Curve 11) [18], GO-Borate (Curve 12) [33], GO-MoS_2-TPU (Curve 13) [17], and GO-Al_2O_3-PVA (Curve 14) [34], respectively. (A colour version of this figure can be viewed online.)

There are two main reasons for the much higher tensile toughness for GO-S-10 as compared with other GO-based artificial nacre. Firstly, the strong π-π stacking interactions between poly (styrene) segments in SSEBS and GO as well as hydrogen bonding interactions between the sulfoacid groups of SSEBS and oxygen-containing groups on the GO surface guarantee strong their interfacial interactions and the effective stress transfer. In other words, adjacent GO nanosheets in our system are interlocked by the physical interactions (π-π stacking and hydrogen bonding), which allows the readily slippage of GO during tension. By contrast, GO-based composites based on chemical bonds including covalent bonds (e.g. GO-GA, GO-PDA, GO-Borate and GO-PCDO) or ionic bonds (GO-Mg^{2+} and GO-Ca^{2+}) can restrict the mutual slippage of GO sheets under external tensile load, thus leading to a much low elongation and tensile toughness despite the high tensile strength. Moreover, the long soft EB segment in SSEBS located in the gallery of layered GO materials tend to deform and extend from the randomly coiled conformation upon loaded, which can absorb much energy and also promote the mutual slippage of GO sheet, thus facilitating the dissipation of fracture energy and leading to a noticeable increase in the tensile toughness. As a result, SSEBS-toughed GO-based artificial nacre shows much higher toughness than other GO-based counterparts with similar structure.

4. Conclusions

Inspired by natural nacre, we created super-tough GO-based artificial nacre via synergistic interface interactions. The synthesized water-soluble sulfonated SEBS copolymer provides numerous functional groups, resulting in formation of π-π interaction and hydrogen bonding with GO nanosheets. This kind of synergistic interface interactions achieves high toughness of 15.3 MJ/m^3, superior to natural nacre and other GO-based nanocomposites. This work provides a novel bioinspired toughening strategy for creating super-tough GO-based nanocomposites.

Acknowledgements

Z. Xu is the co-first author and P. Song and Z. Xu contributed equally to the work.

This work was financially supported by the Natural National Science Foundation of China (51522301, 51303162, 51304166 and 51628302) and the Non-profit Project of Science and Technology Agency of Zhejiang Province of China (Grant No. 2013C32073). P.S. was also supported by an Alfred Deakin Postdoctoral Research Fellowship at Deakin University (Grant No. 0000025468).

Appendix A. Supplementary data

Supplementary data related to this article can be found at http://dx.doi.org/10.1016/j.carbon.2016.10.067.

References

[1] F. Bouville, E. Marire, S. Meille, B. Van de Moortèle, A.J. Stevenson, S. Deville, Strong, tough and stiff bio-inspired ceramics from britle constitutes, Nat. Mater. 13 (2014) 508–514.
[2] Z. Huang, X. Li, Order-disorder transition of aragonite nanoparticles in nacre, Phys. Rev. Lett. 109 (2012) 025501.
[3] J. Wang, Q. Cheng, Z. Tang, Layered nanocomposites inspired by the structure and mechanical properties of nacre, Chem. Soc. Rev. 41 (2012) 1111–1129.
[4] Q.F. Cheng, M. Li, L. Jiang, Z.Y. Tang, Bioinspired layered composites based on flattened double-walled carbon nanotubes, Adv. Mater. 24 (2012) 1838–1843.
[5] A. Finnemore, P. Cunha, T. Shean, S. Vignolini, S. Guldin, M. Oyen, U. Steiner, Biomimetic layer-by-layer assembly of artifical nacre, Nat. Commun. 3 (2012) 966.
[6] X.Q. Li, H.C. Zeng, Calcium carbonate nanotablets: bridging artifical to natural nacre, Adv. Mater. 24 (2012) 6227–6282.
[7] Z. Tang, N.A. Kotov, S. Magonov, B. Ozturk, Nanostructured artifical nacre, Nat. Mater. 2 (2003) 413–418.
[8] P. Podisiadlo, A.K. Kaushik, E.M. Arruda, A.M. Waas, B.S. Shim, J.D. Xu, H. Nandivada, B.G. Pumpplin, J. Lahann, A. Ramamoorthy, et al., Ultrastrong and stiff layed polymer nanocomposites, Science 318 (2007) 80–83.
[9] L.J. Bonderer, A.R. Studart, L.J. Gauckler, Bioinspired design and assembly of platelet reinforced polymer film, Science 319 (2008) 1069–1073.
[10] S. Deville, E. Saiz, R.K. Nalla, A.P. Tomsia, Freezing as a path to build complex composites, Science 311 (2006) 515–518.
[11] H.B. Yao, H.Y. Fang, Z.H. Tan, L.H. Wu, S.H. Yu, Biologically inspired, strong, transparent, and functional layed organic-inorganic hybrid films, Angew. Chem. Int. Ed. 49 (2010) 2140–2145.
[12] Q.F. Cheng, L. Jiang, Z.Y. Tang, Bioinspired layed materials with superior mechanical performance, Acc. Chem. Res. 47 (2014) 1256–1266.
[13] X. Huang, X. Qi, F. Boey, H. Zhang, Graphene-based composites, Chem. Soc. Rev. 41 (2012) 666–686.
[14] D.A. Dikin, S. Stankovih, E.J. Zimney, R.D. Piner, G.H. Dommett, G. Evmenenko, S.T. Nguyen, R.S. Ruoff, Preparation and characterization of graphene oxide paper, Nature 448 (2007) 457–460.
[15] D. Li, R.B. Kaner, Graphene-based materials, Science 320 (2008) 1170–1171.
[16] Q.F. Cheng, M.X. Wu, M.Z. Li, L. Jiang, Z.Y. Tang, Ultratough artifical nacre based on conjugated cross-linked graphene oxide, Angew. Chem. Int. Ed. 52 (2013) 3750–3755.
[17] S.J. Wan, Y.C. Li, J.S. Peng, H. Hu, Q.F. Cheng, L. Jiang, Synergistic toughnening of graphene oxide-molybdenum disulfide-thermoplastic polyurethane ternary artifical nacre, ACS Nano 9 (2015) 708–714.
[18] W. Cui, M.Z. Li, J.Y. Liu, B. Wang, C. Zhang, L. Jiang, Q.F. Cheng, A strong integrated strength and toughness artifical nacre based on dopamine cross-linked graphene oxide, ACS Nano 8 (2014) 9511–9517.
[19] S.Y. Wu, Q.P. Guo, M. Kraska, B. Stühn, Y.-W. Mai, Toughening epoxy thermosets with block ionomers: the role of phase domain size, Macromolecules 46 (2013) 8190–8202.
[20] S.Y. Wu, Q.P. Guo, S.H. Peng, N. Hameed, M. Karaska, B. Stuhn, Y.W. Mai, Toughening epoxy thermosets with block ionomer complexs:a nanostructure-mechanical property correlation, Macromolecules 45 (2012) 3829–3840.
[21] B. Shen, W.T. Zhai, C. Chen, D.D. Lu, J. Wang, W.G. Zheng, Melt blending in situ enhances the interaction between polystyrene and graphene through π-π stacking, ACS Appl. Mater. Interfaces 3 (2011) 3013–3109.
[22] A. Jackson, J. Vincent, R. Yurner, The mechanical design of nacre, Proc. R. Soc. B 234 (1988) 415–440.
[23] P.A. Song, Z.H. Cao, Y.Z. Cai, L.P. Zhao, Z.P. Fang, S.Y. Fu, Fabrication of exfoliated graphene-based polypropylene nanocomposites with enhanced mechanical and thermal properties, Polymer 52 (2011) 4001–4010.
[24] R.A. Weiss, A. Sen, C.L. Willis, L.A. Pottick, Block copolymer Ionomer.1. Synthesis and physical properties of sulfonated poly(styrene ethylene/butylene styrene), Polymer 32 (1991) 1867–1874.
[25] S.Y. Wu, S.H. Peng, N. Hameed, Q.P. Guo, Y.W. Mai, A new route to nanostructured thermosets with block ionomer complexs, Soft Matter 8 (2012) 688–698.
[26] Y. Tian, Y.W. Cao, Y. Wang, W.L. Yang, J.C. Feng, Realizing ultrahigh modulus and high strength of macroscopic graphene oxide papers through crosslinking of mussel-inspired polymers, Adv. Mater. 25 (2013) 2980–2983.
[27] S. Park, K.S. Lee, G. Bozoklu, W. Cai, S.T. Nguyen, R.S. Ruoff, Graphene oxide papers modified by divalent ions-enhancing mechanical properties via chemical cross-linking, ACS Nano 2 (2008) 572–578.
[28] S. Park, D.A. Dikin, S.T. Nguyen, R.S. Ruoff, Graphene oxide sheets chemically cross-linked by polyallylamine, J. Phys. Chem. C 113 (2009) 15801–15804.
[29] Y.Q. Li, T. Yu, T.Y. Yang, L.X. Zheng, K. Liao, Bio-inspired nacre-like composite films based on graphene with superior mechanical, ellectric, and biocompatible properties, Adv. Mater. 24 (2012) 3426–3431.
[30] K.S. Hu, L.S. Tolentino, D.D. Kulkarni, C.H. Ye, S. Kumar, V.V. Tsukruk, Written-in coductive patterns on robust graphene oxide biopaper by electrochemical microstamping, Angew. Chem. Int. Ed. 52 (2013) 13784–13788.
[31] Y. Gao, Y.Q. Liu, S.Z. Zu, K. Peng, D. Zhou, B.H. Han, Z. Zhang, The effect of interlayer adhesion on the mechanical behaviors of macroscopic graphene oxide papers, ACS Nano 5 (2011) 2134–2141.
[32] K.W. Putz, O.C. Compton, M.J. Palmeric, S.T. Nguyen, L.C. Brinson, High-nanofiller-content graphene-polymer nanocomposites via vacuum-assisted self-assembly, Adv. Funct. Mater. 24 (2012) 3426–3431.
[33] Z. An, O.C. Compton, K.W. Putz, L.C. Brinson, S.T. Nguyen, Bio-Inspired borate cross-linking in ultra-stiff graphene oxide thin films, Adv. Mater. 23 (2011) 2980–2983.
[34] J.R. Wang, J.L. Qiao, J.F. Wang, Y. Zhu, L. Jiang, Bioinspired hierarchical alumina-graphene oxide-poly(vinyl alcohol) artificial nacre with optimized strength and toughness, ACS Appl. Mater. Interfaces 7 (2015) 9281–9286.